# Surface modification and retardation of back reaction by nitrogen ion-beam treatment in dye-sensitized solar cells

Sung-Ryong Kim[a,*], Mohammad Al-Mamun[a], Young-Hui Ko[a]

[a]Department of Polymer Science and Engineering, Chungju National University, Chungju 380-702, Republic of Korea

**Abstract**

The photovoltaic performances and charge recombination of the dye sensitized solar cells (DSSCs) using N-modified $TiO_2$ photoelectrodes were investigated under different ion-beam conditions. N-modified $TiO_2$ films exhibited significantly enhanced BET surface area of 92.19 $m^2/g$ with the pore volume of 0.283 $cm^3/g$ compared to the surface area of 56.65 $m^2/g$ with a pore volume of 0.141 $cm^3/g$ of pristine $TiO_2$ film. The interstitial and substitutional affixations of nitrogen atom inside the $TiO_2$ lattice were confirmed by XPS and Raman spectroscopy. A 26% improvement in conversion efficiency was achieved by using $N^+$ ion-beam treated $TiO_2$ photoelectrode.

*Key words*: Ion-beam, Surface modification, DSSCs, Recombination reactions, Raman

* Corresponding author. Tel.: +82 43 8415426; Fax: +82 43 8415420

E-mail address: srkim@ut.ac.kr (Sung-Ryong Kim)

**Highlights:**

- Porous channel for effective dye adsorption by $N^+$ ion-beam treatment
- Effectively tailored surface properties of $TiO_2$ film
- Retardation of charge recombination in dye sensitized solar cells
- Enhanced conversion efficiency of DSSCs by $N^+$ ion-beam treatment.

## 1. Introduction

Grätzel *et.al.* reported a photochemical solar cell using $TiO_2$ nanoparticle sensitized by stable Ru(II)-complex dye in 1991[1]. Due to its simplistic fabrication method and low cost, the dye-sensitized solar cell (DSSC) is proven to be one of the promising candidate for photovoltaic devices [2,3]. Recently, the highest conversion efficiency of DSSS reached at 12.3% using Co(II/III) tris(bipyridal)-based redox electrolyte in conjugation with zinc porphyrin dye [4].

It is well known that $TiO_2$ suffers from the oxygen deficiency with the creation of overall reduced state by forming covalent characteristic suboxides, such as TiO and $Ti_2O_3$. These surface defects are located in the inner band region and cause slow charge transport and higher recombination in DSSCs [5]. Plasma and ion-beam techniques were considered to be effectual surface modification methods to tailor the physical and chemical properties of metal oxide surface. The oxygen ion-beam and plasma treatment were reported to enhance the DSSC performance [6,7]. Nitrogen plasma and ion-beam modified $TiO_2$ films were mostly applied to investigate the photooxidation, photocatalytic conversion and photoreduction in different applications [8,9]. Recently, nitrogen incorporation in $TiO_2$ crystal by chemical wet method became popular for the improvement of photoconversion efficiency in DSSCs [10]. Due to the improved electrical and optical properties of N-modified $TiO_2$ films, it was found to be effective on photocatalytic, photovoltaic and sensor devices applications [11,12]. Nitrogen incorporation in the $TiO_2$ lattice by ion-beam treatment was reported to medicate methylene blue and the degradation was highly dependent on ion energy, ion fluence, irradiation time and the amount of nitrogen content [8]. However, the low energy $N^+$ ion-beam treatment on $TiO_2$ film was not reported for DSSCs.

In this paper, we report $N^+$ ion-beam as an effective treatment to replace the oxygen deficiency in $TiO_2$ lattice. The incorporation of nitrogen atom as a substitutional and

interstitial mode creates adsorption sites for higher dye uptake and retards the charge recombination as well. We suggest that $N^+$ ion-beam treatment is an effective physicochemical method to modify the photo electronic properties of $TiO_2$ surface and consequent improvement of DSSCs parameters.

## 2. Experimental

$TiO_2$ (Ti-Nanoxide D, Solaronix SA) film thickness of around ~8 μm were applied on FTO glass substrate and subjected to $N^+$ ion-beam irradiation using a Kaufman type ion gun under the ion energy of 1000 and 1250 eV with a irradiation pressure of $2.2\times10^{-4}$ Torr. The ion-beam current density and ion fluence was 1.5 mA/cm$^2$ and ~$\times10^{17}$ ions/cm$^2$ respectively. The ion fluence was measured using a custom-built Faraday Cup. The acceleration voltage was 100 V, and the nitrogen gas flow rate was 10 sccm. Under the above condition, the fraction of $N^+$ ion in the extracted beam is predominant [8].

The ion-beam treated $TiO_2$ photoelectrodes were immersed into the dye solution (N719, Ru 535 bis-TBA, Solaronix, SA) for 24 h in the dark and subsequent rinsing with acetonitrile to remove the unanchored dyes. The dried photoelectrodes were sandwiched against a predrilled Pt sputtered counter-electrode filled with electrolyte consisting of 0.5 M LiI, 0.05 M $I_2$, 0.5 M 1,2-dimethyl-3-propylimidazolium iodide and 4-tertbutylpyridine 0.5 M in a mixed solvent of propylene carbonate and acetonitrile (1:4). A DSSC with untreated $TiO_2$ film was also prepared for comparison. The surface morphology of the $TiO_2$ films was observed by field emission scanning electron microscopy (FE-SEM, JSM-6700, JEOL) and the XPS spectra of the $TiO_2$ films were obtained using ESCALAB210 (VG Scientific Ltd., UK). Dispersive-Raman spectrum was measured by Lab RAM HR UV/Vis/NIR, Horiba JobinYvon, France. The BET specific surface area was determined by the level of nitrogen adsorption (BELSOPR II, BEL Japan) at 77 K and the pore size distribution was calculated

using the Barrett, Joyner and Halenda (BJH) method. The contact angle on the$TiO_2$ surface was measured by Phoenix 300 and the UV–Vis spectra of the adsorbed dye on the $TiO_2$ surface were obtained using a UV–Vis spectrophotometer (Hewlett Packard 8453). The DSSCs were illuminated with 100 mW/cm$^2$, AM 1.5 using a 450 W Xe high power arc lamp housing (LH 151, Spectral Energy Co.). The light intensity was calibrated using a Radiometer Photometer (ILT1400-A). The impedance spectra were measured using impedance analyzer (CH Instruments, Inc.) and scanned over the frequency range, $10^{-2}$-$10^5$ Hz.

## 3. **Results and discussion**

Fig. 1 shows FE-SEM images of the $TiO_2$ film surfaces before and after $N^+$ ion-beam irradiation under different ion fluence. It is evident that the pristine $TiO_2$ film having agglomerated particles can retard the effective dye adsorption on $TiO_2$ film. Nitrogen ion-beam irradiation at 1000 and 1250 eV under the ion fluence of $2.13\times10^{17}$ and $0.37\times10^{17}$ ions/ cm$^2$ were sufficient to break the agglomerated $TiO_2$ particles which provide a relatively porous surface, consistent with the previous results [6]. It could be suggested that under the above ion-beam conditions, the critical number of ions having adequate ion-energy could result in the effective morphological changes by removing the organic impurities with increased porosity for better dye penetration inside the bulk of the film. However, the DSSCs prepared with the ion fluence of $1.37\times10^{17}$ ions/cm$^2$ at 1250 eV showed the severely etched porous morphology due to the separation of weakly bonded $TiO_2$ particles and lower conversion efficiency compared to that of $0.37\times10^{17}$ ions/cm$^2$ under the same condition [8,13].

Fig. 2(a) shows the N 1*s* peak for N-modified $TiO_2$ film, a main peak at 399.47 eV and a shoulder peak at 396.91 eV. The peak around 400 eV was mostly assigned as the interstitial

incorporation of nitrogen as N–O or N–N bonding and the peak around 396 eV as the substitutional nitrogen in the form of $N^{3-}$ ion into the $TiO_2$ lattice [14,15]. It suggested the successful attachment of nitrogen in $TiO_2$ lattice in interstitial and substitutional modes. In fig. 2(b), the Ti $2p_{3/2}$ and Ti $2p_{1/2}$ core levels appeared at 458.47, 464.28 eV for pristine and 458.37, 464.04 eV for N-modified $TiO_2$ film. The slight peak shift to lower binding energy can be explained by the change of electron density around Ti atom due to the formation of Ti–N bond with the introduction of nitrogen in $TiO_2$ [15,16]. Also, a small shift of O 1*s* peak (not shown) from 529.75 to 529.59 eV was observed for N-modified $TiO_2$ film which could be attributed to the different atomic environment originated by nitrogen substitution inside the $TiO_2$ lattice [17].

In Fig. 3, there are six Raman active fundamental modes at 143 ($E_g$), 196 ($E_g$), 396 ($B_{1g}$), 516 ($A_{1g}$ + $B_{1g}$), and 640 $cm^{-1}$ ($E_g$) [18,19]. The existence of anatase phase of $TiO_2$ after $N^+$ ion-beam treatment could be confirmed by three principal peaks arisen at around 396.10 $cm^{-1}$ ($B_{1g}$), 515.70 $cm^{-1}$ ($A_{1g}$), and 639.63 $cm^{-1}$ ($E_g$). Comparing the lowest anatase characteristic peak at around 143 $cm^{-1}$ (inset) of the untreated and the ion-beam treated sample showed significant increase of intensity, width and slight peak position shift from 142.79 to 143.16 $cm^{-1}$ which indicated the assuredly substituted nitrogen for some oxygen atoms in titania lattice [16].

The hydrophilicity of N-modified $TiO_2$ film was investigated by water contact angle measurement. The water contact angle of the untreated $TiO_2$ film was 17.89°, which decreased to 9.15° upon $N^+$ ion-beam treatment and it was maintained even after 72 h. It suggested the retention of high surface energy of N-modified $TiO_2$ film for a considerable amount of time. The hydrophilic surface with low water contact angle could interact more strongly with the carboxylic groups present in the dye and result in higher dye uptake [20].

Fig. 4 (a) shows the BET isotherms and pore size distributions (inset) of pristine $TiO_2$ film and N-modified $TiO_2$ film under different condition. BET specific surface area of pristine $TiO_2$ film was calculated to be 56.65 $m^2/g$ with a pore volume and average pore diameter of 0.141 $cm^3/g$ and 9.97 nm, respectively. After $N^+$ ion-beam treatment under the ion fluence of $0.37\times10^{17}$ ions/$cm^2$ at 1250 eV, the BET specific surface area of the $TiO_2$ film was significantly increased to 92.19 $m^2/g$ with a pore volume of 0.279 $cm^3/g$ and pore diameter of 12.12 nm. Fig. 4(b) shows the UV-Vis spectra of N719 desorbed from $TiO_2$ photoelectrodes, dye adsorption was increased by 25.93% at 500 nm for N-modified $TiO_2$ film under the ion fluence of $0.37\times10^{17}$ ions/$cm^2$ at 1250 eV. The higher dye adsorption is related to the presence of $N^{3-}$ ion in the $TiO_2$ lattice which can oxidize the $Ti^{3+}$ center to $Ti^{4+}$. The higher charge on Ti was expected to interact more strongly with the carboxylic group of dye [21].

Fig. 5(a) shows the photocurrent–voltage characteristics of the DSSCs based on the pristine and N-modified $TiO_2$film at 1000 and 1250 eV. N-modified DSSCs showed only 10 mV increase of open circuit voltage ($V_{oc}$'s) which may be related to the similar band gap even after $N^{3-}$ incorporation in $TiO_2$ lattice [22]. But significant increase of short circuit current ($J_{sc}$) were observed after $N^+$ ion-beam treatment from the initial value of 11.88 to 14.57 mA/ $cm^2$. The increased short circuit density ($J_{sc}$) was related to higher dye uptake as result of physicochemical modification of $TiO_2$ surface by $N^+$ ion-beam treatment. No significant change in fill factors (FF) was observed after $N^+$ ion-beam treatment on photoanode. Also, DSSCs prepared by N-modified $TiO_2$ photoelectrode under the ion fluence of $0.37\times10^{17}$ ions/ $cm^2$ at 1250 eV reached the maximum conversion efficiency up to 6.96% from 5.53% of the pristine one.

The significantly increased radius of the mid-semicircle regime in Fig. 5(b) resembles the augmented surface resistance of $TiO_2$ photoelectrode and suppressed back-transfer of photogenerated electrons of N-modified $TiO_2$ films to the electrolyte at $TiO_2$/dye/electrolyte interface. From Bode phase plots, increased amplitude and electron lifetime were also observed. The DSSCs prepared under the ion fluence of $0.37\times10^{17}$ions/cm$^2$ at 1250 eV showed lower charge recombination and higher electron lifetime from 34.84 to 39.51 ms compared to pristine $TiO_2$. $N^+$ ion-beam treated DSSCs also showed suppressed production of dark current compare to untreated one. It is evident that when a negative potential is applied between the photoanode and counter electrode, the electrons are forced to transfer and trapped by different pathways. Figure (S.1) illustrates the comparative dark current of DSSCs based on $N^+$ ion-beam treated and untreated $TiO_2$ photo electrodes. The $N^+$ ion-beam treated DSSCs exhibit smaller dark current, which indicates that nitrogen incorporation could successfully retard the charge recombination at $TiO_2$/dye/electrolyte interface. Thus, the bond O–Ti–N, formed by $N^+$ ion-beam treatment could effectively inhibit the reduction of $I^{3-}$ on the $TiO_2$ electrode [17].

The surface defects originated from the oxygen deficiency in $TiO_2$ lattice lead to the formation of paramagnetic center which act as a trap sites for photogenerated electrons in $TiO_2$ surface [23]. $N^+$ ion-beam treatment introduces N as a preferred state of $N^{3-}$ inside the lattice which can oxidize the reduced state of $Ti^{3+}$ to $Ti^{4+}$ by filling the N-2p state [24]. This causes the depletion of the Ti 3d state and removes the trapping centers for photogenerated electrons [22]. The surface modification of $TiO_2$ films by $N^+$ ion-beam treatment improved the surface properties, electron lifetime, and retardation of charge recombination in DSSCs.

## 4. Conclusions

$N^+$ ion-beam treatment was employed to increase the surface area and porosity of $TiO_2$ film and to reduce the charge recombination of DSSCs. XPS and Raman spectra revealed the presence of nitrogen inside the $TiO_2$ lattice as interstitial and substitutional states. It is speculated that the introduction of nitrogen as $N^{3-}$ ion replaced the oxygen deficiencies in the $TiO_2$ lattice and lead to the smaller number of surface defects. Electrochemical impedance spectroscopy results indicated the appreciable decrease in recombination reaction after $N^+$ ion-beam treatment. The effective reduction of surface defects resulted in lesser recombination and longer electron lifetime in DSSCs. We found the increase of photo-conversion efficiency by 26% which is quite significant for the development of high performance DSSCs. This paper demonstrates the effectiveness of the $N^+$ ion-beam treatment to tailor the defect sites, surface properties and the consequent improvement of DSSCs performance.

**Acknowledgements**

This research was financially supported through the Human Resource Training Project for Regional Innovation and Grant (2010-0006808) by the Ministry of Education, Science Technology of Korea. Also, this work was supported by National Research Foundation of Korea Grant funded by the Korean Government 2010-0006808 and by a grant from the Academic Research Program of Korea National University of Transportation in 2012.

**References**


[1] B. O'Regan, M. Gratzel, Nature 353 (1991) 737.

[2] A. Kay, M. Grätzel, Solar Energy Mater. Solar Cells 44 (1996) 99.

[3] S.R. Kim, M.K. Parvez, I. In, H.Y. Lee, J.M. Park, Electrochim. Acta 54 (2009) 6306.

[4] A. Yella, H. Lee, H.N. Tsao, C. Yi, A.K. Chandiran, M.K. Nazeeruddin, E.W. Diau, C. Yeh, S.M. Zakeeruddin, M. Grätzel, Science 334 (2011) 629.

[5] H. Wang, J. Hen, G. Boschloo, H. Lindström, A. Hagfeldt, S. Lindquist, J. Phys. Chem. 105 (2001) 2529.

[6] M.K. Parvez, G.M. Yoo, J.H. Kim, M.J. Ko, S.R. Kim, Chemical Physics Letters 495 (2010) 69.

[7] S.R. Kim, M.K. Parvez, J. Mater. Res. 26 (2011) 1012.

[8] H. Shen, L. Mi, P. Xu, W. Shen, P. Wang, Appl. Surf. Sci. 253 (2007) 7024.

[9] T. Yuji, H. Akatsuka, N. Mungkung, B.W. Park, Y.M. Sung, Vacuum 83 (2008) 124.

[10] W. Guo, Y. Shen, L. Wu, Y. Gao, T. Ma, J. Phys. Chem. C 115 (2011) 21494.

[11] T. Narita, T. Iida, S. Ogawa, K. Mizuno, J. So, A. Kondo, N. Yoshida, T. Itoh, S. Nonomura, Y. Tanaka, Thin Solid Films 516 (2008) 810.

[12] S.E. Gledhill, B. Scott, B.A. Gregg, J. Mater. Res. 20 (2005) 3167.

[13] L. Liang, S. Dai, L. Hu, F. Kong, W. Xu, K. Wang, J. Phys. Chem. B 110 (2006) 12404.

[14] R. Asahi, T. Morikawa, T. Ohwaki, K. Aoki, Y. Taga, Science 293 (2001) 269.

[15] J. Wang, W. Zhu, Y. Zhang, S. Liu, J. Phys. Chem. C 111 (2007) 1010.

[16] X. Chen, C. Burda, J. Phys. Chem. B 108 (2004) 15446.

[17] H. Tian, L. Hu, C. Zhang, W. Liu, Y. Huang, L. Mo, L. Guo, J. Sheng, S. Dai, J. Phys. Chem. C 114 (2010) 1627.

[18] Y. Huo, Z. Bian, X. Zhang, Y. Jin, J. Zhu, H. Li, J. Phys. Chem. C 112 (2008) 6546.

[19] Y. Cong, J. Zhang, F. Chen, M. Anpo, J. Phys. Chem. C 111 (2007) 6976.

[20] K. Pomoni, A. Vomvas, C. Trapalis, J. Non Cryst. Solids 354 (2008) 4448.

[21] M. Aizawa, Y. Morikawa, Y. Namai, H. Morikawa, Y. Iwasawa , J. Phys. Chem. B 109 (2005) 18831.

[22] M. Batzill, Phys. Rev. Lett 96 (2006) 026103.

[23] G. Pacchioni, ChemPhysChem 4 (2003) 1041.

[24] M. Batzill, E.H. Morales, U. Diebold, Chem. Phys. 339 (2007) 36.

**Table 1**
Characteristics of the DSSCs with the pristine and N-modified $TiO_2$ photoelectrodes.

| $TiO_2$ films | Ion fluence ($\times 10^{17}$ ions/cm$^2$) | Dye adsorbed ($\times 10^{-5}$ mol/cm$^2$) | $V_{oc}$ (V) | $J_{sc}$ (mA/cm$^2$) | *FF* (%) | $\eta$ (%) |
|---|---|---|---|---|---|---|
| Untreated | - | 3.78 | 0.73 | 11.88 | 63.71 | 5.53 |
| Ion-beam energy | 1.07 | 4.29 | 0.73 | 12.12 | 64.34 | 5.71 |
| (1000 eV) | 2.13 | 4.41 | 0.74 | 13.99 | 65.05 | 6.75 |
| Ion-beam energy | 0.37 | 4.76 | 0.74 | 14.57 | 64.55 | 6.96 |
| (1250 eV) | 1.37 | 4.43 | 0.73 | 12.44 | 63.06 | 5.70 |

**Figure Captions**

**Fig. 1.** Field emission scanning electron microscopy images of (a) pristine, (b) 1000 eV ($2.13\times 10^{17}$ ions/cm$^2$), and (c) 1250 eV ($0.37\times10^{17}$ ions/ cm$^2$) $N^+$ ion-beam treated $TiO_2$ film surface.

**Fig. 2.** XPS spectrum of (a) N 1*s* peak of N-modified and (b) Ti 2*p* of pristine and modified $TiO_2$ films.

**Fig. 3.** Raman spectra of full length and expanded for $E_g$ mode (inset) at 143 cm$^{-1}$ of pristine and N-modified $TiO_2$ film.

**Fig. 4.** (a) Nitrogen gas adsorption-desorption isotherm and pore size distribution (inset) and (b) absorption spectra of N719 dye desorbed from untreated and ion-beam treated $TiO_2$ films.

**Fig. 5.** (a) *J-V* characteristic curve (b) Nyquist plots for DSSC based on pristine and N-modified $TiO_2$ photoelectrodes.

**Figure 1**

Click here to download high resolution image

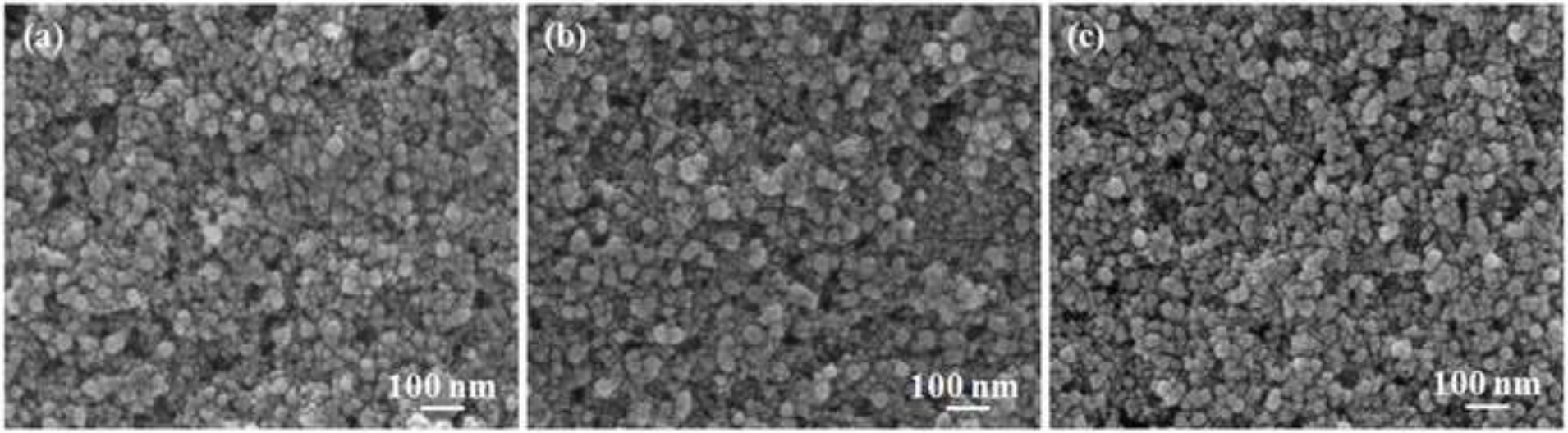

Figure 2

Click here to download high resolution image

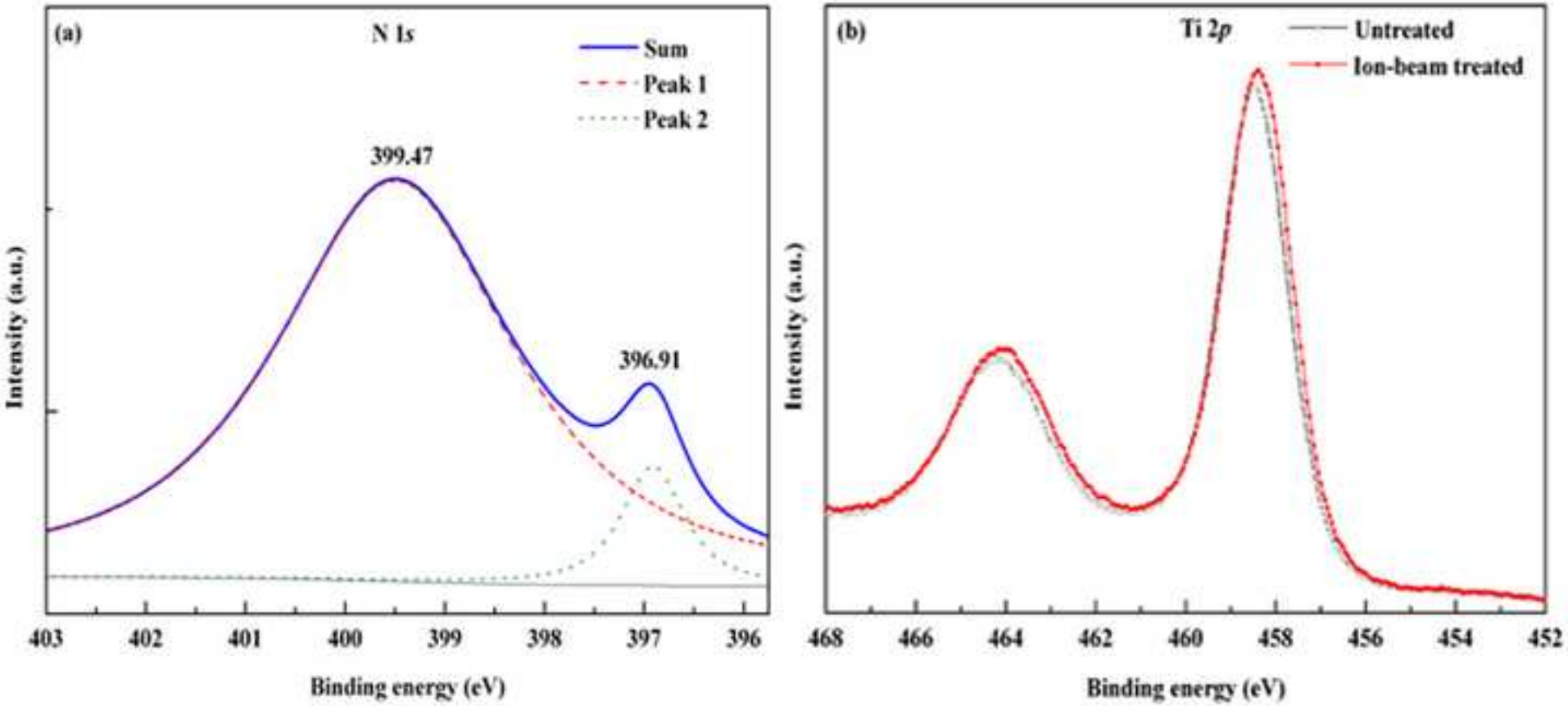

Figure 3

Click here to download high resolution image

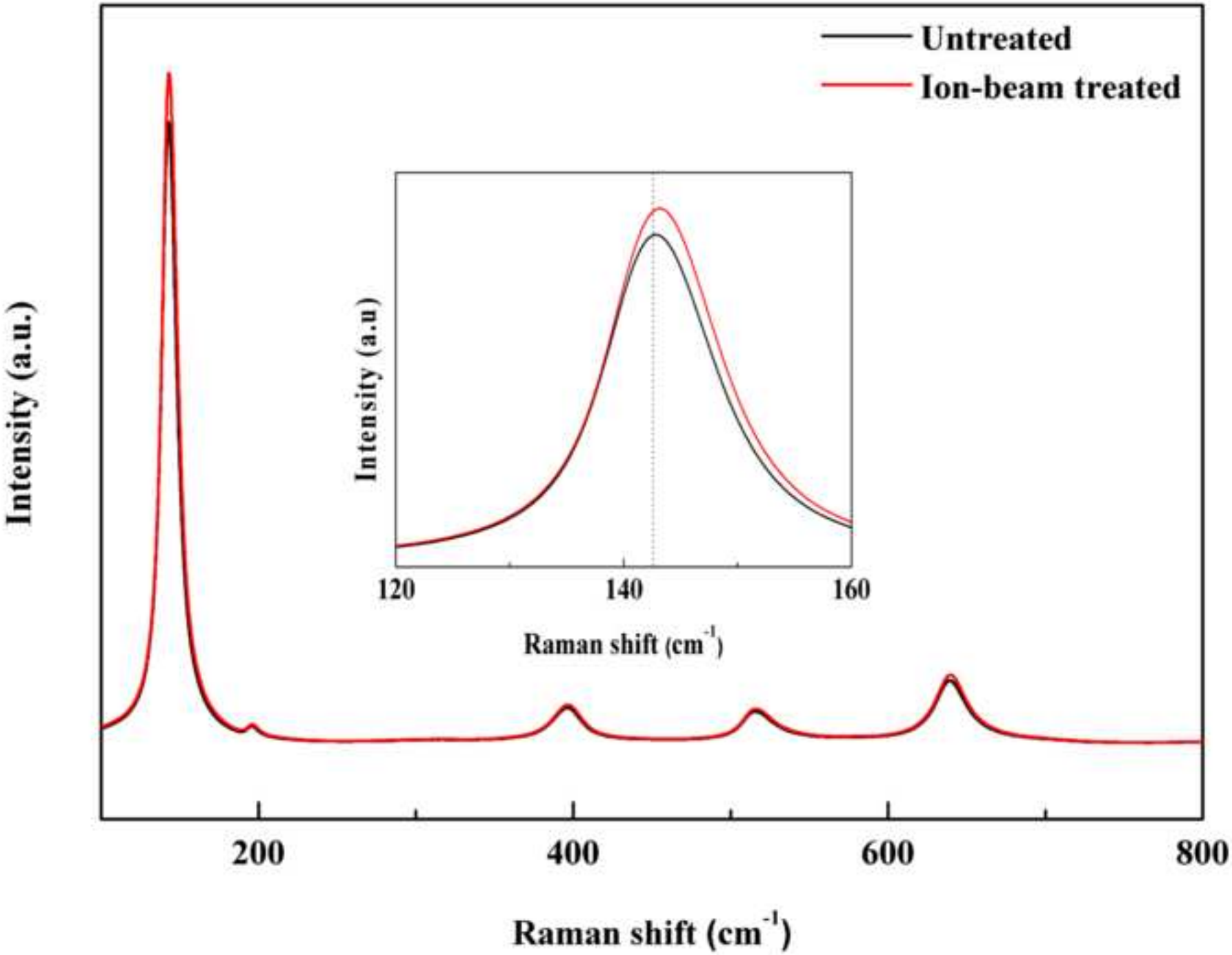

Figure 4

Click here to download high resolution image

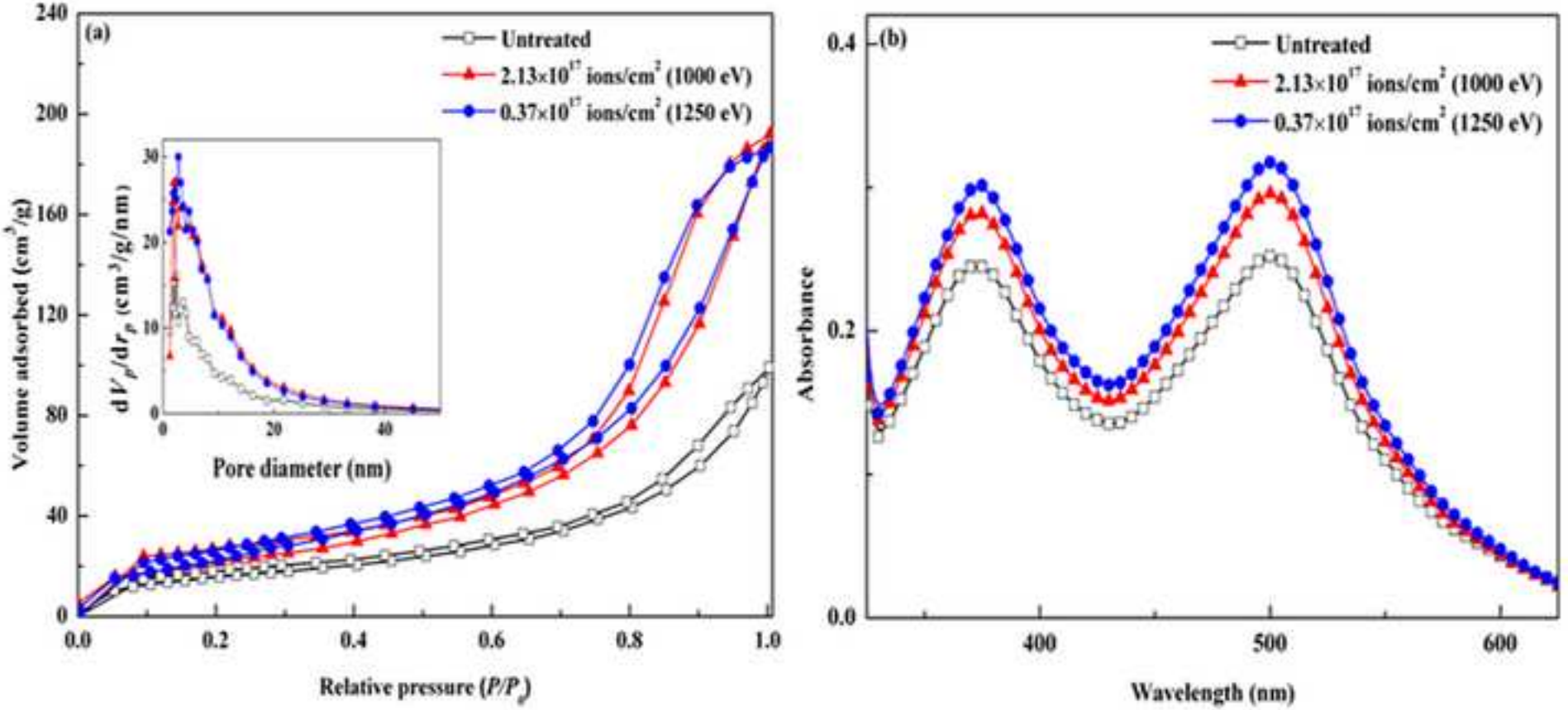

Figure 5

Click here to download high resolution image